

Nonlinear Elasticity for Modeling Fracture of Isotropic Brittle Solids

K. Y. Volokh

Faculty of Civil and Environmental Engineering,
Technion, Haifa 32000, Israel

A softening hyperelastic continuum model is proposed for analysis of brittle fracture. Isotropic material is characterized by two standard parameters—shear and bulk modulus—and an additional parameter of the volumetric separation work. The model can be considered as a volumetric generalization of the concept of the cohesive surface. The meaning of the proposed constitutive equations is clarified by the examples of simple shear and hydrostatic pressure. It is emphasized that the proposed constitutive model includes only smooth functions and the necessary computational techniques are those of nonlinear elasticity. [DOI: 10.1115/1.1636795]

1 Introduction

The idea to describe fracture as a material separation across a surface was pioneered by Barenblatt [1]. It appears by name of the cohesive zone model (CZM) in the modern literature. The cohesive zone is a surface in a bulk material where displacement discontinuities occur. Thus, continuum is enhanced with discontinuities. The latter requires an additional constitutive description. Equations relating normal and tangential displacement jumps across the cohesive surfaces with the proper tractions define a specific CZM. There is a plenty of proposals of the “cohesive” constitutive equations (for example, Barenblatt [1], Rice and Wang [2], Tvergaard and Hutchinson [3], and Xu and Needleman [4]). All these models are constructed qualitatively as follows: tractions increase, reach a maximum, and then approach zero with increasing separation. This scenario is in harmony with our intuitive understanding of the rupture process. It is qualitatively analogous to atomic interactions.

Needleman [5] lifted the cohesive zone models to computational practice. Since then CZMs are used increasingly in finite element simulations of crack-tip plasticity and creep; crazing in polymers; adhesively bonded joints; interface cracks in bimetals; delamination in composites and multilayers; fast crack propagation in polymers, etc. Cohesive zones can be inside finite elements or along their boundaries (de Borst [6], Xu and Needleman [4], and Belytschko et al. [7]). Crack nucleation, propagation, branching, kinking, and arrest are a natural outcome of the computations where the discontinuity surfaces are spread over the bulk material. This is in contrast to the traditional approach of fracture mechanics where stress analysis is separated from a description of the actual process of material failure.

The CZM approach is natural for simulation of fracture at the material interface in composites and multilayers. It is less natural for modeling fracture of the bulk material because it leads to the simultaneous use of two material models for the same real material. One model describes the bulk material, while the other model describes the cohesive zones imbedded in the bulk material. Such two-model approach is rather artificial physically. It seems preferable to incorporate a material failure law directly in the constitutive description of the bulk material. Such volumetric models of the material failure via strain localization are usually based on inelastic constitutive equations, including damage theories, where

the strain softening takes place (see the survey article by de Borst [6]). An interesting hyperelastic softening model based on the microstructural concept of the virtual internal bond has been proposed recently by Gao and Klein [8].

The computational efficiency of both volumetric and surface fracture models can suffer from two general problems. The first problem is mesh sensitivity. It takes place when the deformed finite element model reaches a critical point, which is a limit and multiple bifurcation point. This happens when a number of finite elements in various areas of the structure reach the cohesive strength simultaneously. The multiplicity of the bifurcation point and, consequently, the sensitivity of computations increase with the refinement of the mesh. The mesh refinement can be limited by introducing the characteristic length like in Bazant and Planas [9] or Gao and Ji [10]. This will provide the upper bound for the bifurcation multiplicity. It does not resolve the problem of the bifurcation multiplicity as a whole, however. A more radical way in circumventing the mesh sensitivity issue is the introduction of the second displacement gradients and conjugate higher order stresses (de Borst and van der Giessen [11] and Hutchinson [12]). This augmented initial boundary value problem can avoid the troubling critical point of the finite element model at all. The price for that is high because the enhanced model requires the additional boundary conditions which are not readily interpreted in simple physical terms.

The bifurcation multiplicity and the related mesh sensitivity are inherent in *any* softening material model for a *specific* loading of the considered structure. Another computational problem of the separation constitutive models is more universal. It is related to the use of inequalities, like in damage or plasticity theories, and vertex—hidden bifurcation—points, like in some compound elastic models of debonding. These undesirable features significantly sophisticate numerical procedures and require informal experience from their user.

We aim at formulating a volumetric material failure model, which is both analytically and computationally simpler than the existing fracture models. For this purpose a nonlinear softening hyperelastic continuum model is considered. Isotropic material is characterized by two standard parameters—shear and bulk modulus—and an additional parameter of the *volumetric separation work*. This model can be considered as a volumetric generalization of the concept of the cohesive surface. The meaning of the proposed constitutive equations is clarified by the examples of simple shear and hydrostatic pressure. It is emphasized that the proposed constitutive model includes only smooth functions and the necessary computational techniques are those of nonlinear elasticity.

2 Constitutive Equations

We set the strain energy per unit volume in the form

$$W = \Phi - \Phi \left(1 + 3 \sqrt{\frac{K}{\Phi}} \varepsilon \right) \exp \left\{ -3 \sqrt{\frac{K}{\Phi}} \varepsilon - \frac{G}{\Phi} e_{ij} e_{ij} \right\}, \quad (2.1)$$

where the standard volumetric/deviatoric decomposition of the strain tensor is used,

$$\varepsilon = \varepsilon_{ii}/3, \quad (2.2)$$

$$e_{ij} = \varepsilon_{ij} - \varepsilon \delta_{ij}. \quad (2.3)$$

Coefficients K and G are the usual bulk and shear modulus respectively, while Φ is a new constant of the isotropic brittle solid. This is the *volumetric separation work*. Its dimension is work per unit volume, i.e., it is the same as the dimension of K and G and the dimension of stress. It is worth emphasizing that the introduced volumetric separation work is different from the separation work traditionally used in the cohesive surface approach to fracture. The dimension of the latter is work per unit area.

For a hyperelastic material stresses are defined as follows:

Contributed by the Applied Mechanics Division of THE AMERICAN SOCIETY OF MECHANICAL ENGINEERS for publication in the ASME JOURNAL OF APPLIED MECHANICS. Manuscript received by the ASME Applied Mechanics Division, October 21, 2002; final revision, August 18, 2003. Associate Editor: H. Gao.

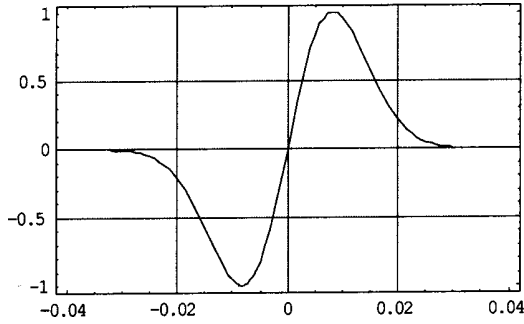


Fig. 1 Simple shear. Normalized traction (vertical axis) versus shear deformation (horizontal axis) as defined by Eq. (3.7).

$$\sigma_{ij} = \frac{\partial W}{\partial \varepsilon_{ij}} = \frac{\partial W}{\partial e_{mn}} \frac{\partial e_{mn}}{\partial \varepsilon_{ij}} + \frac{\partial W}{\partial \varepsilon} \frac{\partial \varepsilon}{\partial \varepsilon_{ij}}. \quad (2.4)$$

All entries on the right-hand side of this equation are readily computed accounting for the strain energy expression:

$$\frac{\partial W}{\partial e_{mn}} = 2Ge_{mn} \left(1 + 3 \sqrt{\frac{K}{\Phi}} \varepsilon \right) \exp \left\{ -3 \sqrt{\frac{K}{\Phi}} \varepsilon - \frac{G}{\Phi} e_{ij} e_{ij} \right\}, \quad (2.5)$$

$$\frac{\partial e_{mn}}{\partial \varepsilon_{ij}} = \delta_{mi} \delta_{jn} - \delta_{ij} \delta_{mn} / 3, \quad (2.6)$$

$$\frac{\partial W}{\partial \varepsilon} = 9K\varepsilon \exp \left\{ -3 \sqrt{\frac{K}{\Phi}} \varepsilon - \frac{G}{\Phi} e_{ij} e_{ij} \right\}, \quad (2.7)$$

$$\frac{\partial \varepsilon}{\partial \varepsilon_{ij}} = \delta_{ij} / 3. \quad (2.8)$$

By using the volumetric/deviatoric decomposition of the stress tensor,

$$\sigma_{ij} = \sigma \delta_{ij} + s_{ij} \quad , \quad \sigma = \sigma_{kk} / 3, \quad (2.9)$$

we have

$$s_{ij} = \frac{\partial W}{\partial e_{ij}} = 2Ge_{ij} \left(1 + 3 \sqrt{\frac{K}{\Phi}} \varepsilon \right) \exp \left\{ -3 \sqrt{\frac{K}{\Phi}} \varepsilon - \frac{G}{\Phi} e_{mn} e_{mn} \right\}, \quad (2.10)$$

$$\sigma = \frac{\partial W}{3 \partial \varepsilon} = 3K\varepsilon \exp \left\{ -3 \sqrt{\frac{K}{\Phi}} \varepsilon - \frac{G}{\Phi} e_{mn} e_{mn} \right\}. \quad (2.11)$$

Linearized Eqs. (2.10) and (2.11) present the classical Hooke's law.

In order to justify and clarify the specific choice of the strain energy we consider two limit cases in the following two sections.

3 Simple Shear

Assume that only the following strain and stress components are nonzero:

$$\tau = s_{12} = s_{21} \quad , \quad \gamma = e_{12} = e_{21}. \quad (3.1)$$

In this case the constitutive law (2.10) takes the form

$$\tau = 2G\gamma \exp \left\{ -\frac{2G}{\Phi} \gamma^2 \right\}. \quad (3.2)$$

The shape of this curve appears in Fig. 1. Qualitatively, this means that the magnitude of the shear traction increases linearly with the shear strain, reaches a maximum, and then approaches zero with increasing separation. It does not matter what the sign of the traction is.

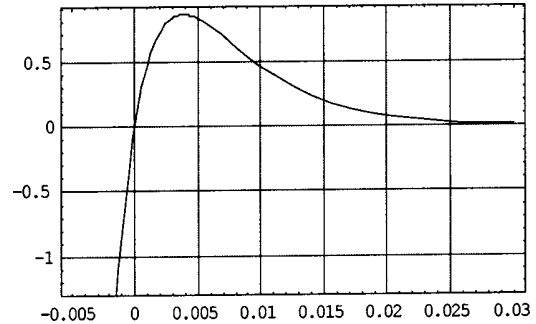


Fig. 2 Hydrostatic pressure. Normalized pressure (vertical axis) versus volumetric deformation (horizontal axis) as defined by Eq. (4.3).

The local maximum of the curve is at point

$$\gamma = \pm \sqrt{\frac{\Phi}{4G}}. \quad (3.3)$$

The corresponding absolute magnitude of the maximum traction is

$$\tau_{\max} = \sqrt{G\Phi} \exp\{-1/2\}. \quad (3.4)$$

Assume that for the given material the maximum traction is known:

$$\tau_{\max} = G/100. \quad (3.5)$$

Then we have

$$\Phi = \frac{G}{10^4 \exp(-1)}. \quad (3.6)$$

Substituting Eq. (3.6) in Eq. (3.2) and normalizing the latter with respect to τ_{\max} we obtain

$$\frac{\tau}{\tau_{\max}} = 200\gamma \exp\{-2 \cdot 10^4 \exp(-1)\gamma^2\}. \quad (3.7)$$

The graph of this function is shown in Fig. 1.

4 Hydrostatic Pressure

Assume that the deformation under a uniform hydrostatic pressure is purely volumetric

$$\sigma_{ij} = \sigma \delta_{ij} \quad , \quad \varepsilon_{ij} = \varepsilon \delta_{ij}. \quad (4.1)$$

In this case the constitutive law (2.11) takes the form

$$\sigma = 3K\varepsilon \exp \left\{ -3 \sqrt{\frac{K}{\Phi}} \varepsilon \right\}. \quad (4.2)$$

The shape of this curve appears in Fig. 2. Qualitatively, it can be interpreted as the linear increase of the magnitude of the tension pressure with the increase of the material volume at the point, it reaches a maximum, and then approaches zero with increasing separation. The latter is nothing but the void nucleation. For the compression pressure the situation is different, however. There is no separation!

Assume that the material is defined by Eq. (3.5) and $K/G=2$, then Eq. (4.2) normalized with respect to τ_{\max} takes the following form:

$$\frac{\sigma}{\tau_{\max}} = 600\varepsilon \exp\{-300\sqrt{2} \exp(-1)\varepsilon\}. \quad (4.3)$$

The graph of this function is shown in Fig. 2.

5 Conclusions

A novel constitutive model of an isotropic brittle solid has been proposed. The exponential hyperelastic constitutive law describes this model. The material bulk modulus and the shear modulus are completed with a new constant—the volumetric separation work. The proposed constitutive equations are cohesive, that is they naturally allow for the material separation–strain localization. These equations may be interpreted on the basis of the simple shear and hydrostatic pressure examples. The distortional (deviatoric) deformation at the given point exhibits behavior analogous to the simple shear, which graph is shown in Fig. 1. The dilatational (volumetric) deformation at the given point exhibits behavior analogous to the hydrostatic pressure, which graph is shown in Fig. 2.

Adding the momentum conservation laws and the proper boundary and initial conditions to the constitutive equations described in Section 2 of our work, it is possible to set the initial boundary value problem of *nonlinear elasticity*. The latter means that the standard and well established numerical procedures are available. When a brittle solid is loaded quasi-statically then the crack nucleation means passing a limit point in the state space of the discretized IBVP. Well-developed techniques of the arc-length continuation can be used (Crisfield [13] and Riks [14]). The loss of the positive definiteness of the tangent stiffness matrix (the Jacobian of the total discrete energy) means static instability. If the equilibrium path does not become stable again, then the dynamic crack propagation takes place and dynamic integration procedures should be used (Belytschko et al. [15] and Xu and Needleman [4]). It is worth emphasizing that only smooth functions are used in the constitutive equations. The latter allows for circumventing the problems of inequalities and vertex points, which are typical of most separation models.

Acknowledgment

This research was supported by the Fund for the Promotion of Research at the Technion.

References

- [1] Barenblatt, G. I., 1959, "The Formation of Equilibrium Cracks During Brittle Fracture—General Ideas and Hypotheses. Axially Symmetric Cracks," *J. Appl. Math. Mech.*, **23**, pp. 622–636.
- [2] Rice, J. R., and Wang, J. S., 1989, "Embrittlement of Interfaces by Solute Segregation," *Mater. Sci. Eng., A*, **107**, pp. 23–40.
- [3] Tvergaard, V., and Hutchinson, J. W., 1992, "The Relation Between Crack Growth Resistance and Fracture Process Parameters in Elastic-Plastic Solids," *J. Mech. Phys. Solids*, **40**, pp. 1377–1397.
- [4] Xu, X. P., and Needleman, A., 1994, "Numerical Simulations of Fast Crack Growth in Brittle Solids," *J. Mech. Phys. Solids*, **42**, pp. 1397–1434.
- [5] Needleman, A., 1987, "A Continuum Model for Void Nucleation by Inclusion Debonding," *ASME J. Appl. Mech.*, **54**, pp. 525–531.
- [6] de Borst, R., 2001, "Some Recent Issues in Computational Failure Mechanics," *Int. J. Numer. Methods Eng.*, **52**, pp. 63–95.
- [7] Belytschko, T., Moes, N., Usiu, S., and Parimi, C., 2001, "Arbitrary Discontinuities in Finite Elements," *Int. J. Numer. Methods Eng.*, **50**, pp. 993–1013.
- [8] Gao, H., and Klein, P., 1998, "Numerical Simulation of Crack Growth in an Isotropic Solid With Randomized Internal Cohesive Bonds," *J. Mech. Phys. Solids*, **46**, pp. 187–218.
- [9] Bazant, Z. P., and Planas, J., 1998, *Fracture and Size Effect of Concrete and Other Quasibrittle Materials*, CRC Press, Boca Raton, FL.
- [10] Gao, H., and Ji, B., 2003, "Modeling Fracture of Nanomaterials via a Virtual Internal Bond Method," *Eng. Fract. Mech.*, **70**, pp. 1777–1791.
- [11] de Borst, R., and van der Giessen, E., 1998, *Material Instabilities in Solids*, John Wiley and Sons, Chichester, UK.
- [12] Hutchinson, J. W., 2000, "Plasticity at the Micron Scale," *Int. J. Solids Struct.*, **37**, pp. 225–238.
- [13] Crisfield, M. A., 1991, 1997, *Non-linear Finite Element Analysis of Solids and Structures*, Vols. 1, 2, John Wiley and Sons, Chichester, UK.
- [14] Riks, E., 1998, "Buckling Analysis of Elastic Structures: A Computational Approach," *Adv. Appl. Mech.*, **34**, pp. 1–76.
- [15] Belytschko, T., Liu, W. K., and Moran, B., 2000, *Nonlinear Finite Elements for Continua and Structures*, John Wiley and Sons, New York.

Flutter of Rotating Shells With a Co-rotating Axial Flow¹

L. Cortelezzi

A. Pong

M. P. Păidoussis

Fellow ASME

Department of Mechanical Engineering, McGill University, Montreal, QC H3A 2K6, Canada

It is shown that, in certain regions of parameter space, travelling wave solutions in rotating shells containing co-rotating inviscid fluid become indeterminate. This may render the determination of the flutter speed impossible, or the solution nonphysical.

[DOI: 10.1115/1.1636794]

Introduction

The dynamics and stability of a shell containing fluid in matched (solid body) rotation and also flowing axially was examined by Lai and Chow [1], inspired by fluid-structure interactions in "the thrust chamber and the pipelines in the liquid propellant feed system of a spinning rocket." In contrast to Srinivasan [2], Dowell et al. [3] and related studies which are connected to a real system and need to face the complications attendant thereto, the problem studied by Lai and Chow is very idealized. A closely similar study was made by Chen and Bert [4] in which the shell is stationary but the fluid is rotating as in the foregoing; thus, the physical system is closer to engineering applications, but the use of inviscid flow theory is less justifiable—see Păidoussis [5] for a review.

This note presents new results which show that some of those by Lai and Chow and Bert and Chen are questionable.

Equations of Motion and Analysis

Consider both the shell and the fluid to be rotating with angular velocity Ω , and the fluid to have an axial velocity U , relative to the shell. The shell is assumed to be very thin and its motions to be governed by the Donnell equations, [1], which in operator form in terms of coordinates rotating with the shell are

$$\mathbf{L}_D \begin{Bmatrix} u \\ v \\ w \end{Bmatrix} = \gamma \begin{Bmatrix} \partial^2 u / \partial t^2 \\ \partial^2 v / \partial t^2 - \Omega^2 v + 2\Omega(\partial w / \partial t) \\ -\partial^2 w / \partial t^2 + \Omega^2 w + 2\Omega(\partial v / \partial t) + p / \rho_s h \end{Bmatrix}, \quad (1)$$

where u , v , and w are the axial, circumferential, and radial displacements of the shell, and the other symbols are as in standard thin-shell theory. The fluid velocities, v_x , v_r , and v_θ , are related to the pressure p by

$$\begin{aligned} \frac{Dv_x}{Dt} &= -\frac{1}{\rho} \frac{\partial p}{\partial x}, \\ \frac{Dv_r}{Dt} - \frac{v_\theta^2}{r} - 2\Omega v_\theta - \Omega^2 r &= -\frac{1}{\rho} \frac{\partial p}{\partial r}, \end{aligned} \quad (2)$$

¹This work was supported by the Natural Sciences and Engineering Research Council of Canada and FCAR of Québec.

Contributed by the Applied Mechanics Division of THE AMERICAN SOCIETY OF MECHANICAL ENGINEERS for publication in the ASME JOURNAL OF APPLIED MECHANICS. Manuscript received by the ASME Applied Mechanics Division, January 16, 2003; final revision, June 9, 2003. Associate Editor: R. C. Benson.